Planetary and Space Science 152 (2018) 176–185

Contents lists available at ScienceDirect

Planetary and Space Science

journal homepage: www.elsevier.com/locate/pss

Space weather at planet Venus during the forthcoming BepiColombo flybys

S. McKenna-Lawlor [a,*], B. Jackson [b], D. Odstrcil [c]

[a] Space Technology Ireland, Ltd., NUI Maynooth, Co. Kildare, Ireland
[b] University of California San Diego, 9500 Gilman Drive, La Jolla 92093, CA, USA
[c] Goddard Space Flight Centre, 8800 Greenbelt Rd., Maryland 20771, USA

ARTICLE INFO

Keywords:
Interplanetary scintillation technique
ENLIL modelling
Coronal mass ejections
Mercury
BepiColombo mission

ABSTRACT

The BepiColombo (BC) Mission which will be launched in 2018, will include during its Cruise Phase two flybys of Venus and five Mercury flybys. It will then enter a one Earth year orbit about Mercury (with a possible one-year extension) during which two spacecraft, one provided by ESA (MPO) and one provided by JAXA (MMO), will perform both autonomous and coordinated observations of the Hermean environment at various separations. The measurements will take place during the minimum of solar cycle 24 and the rise of solar cycle 25. At the start of the minimum of solar cycle 23, four major flares, each associated with the production of MeV particle radiation and CME activity occurred. Predictions of the HAFv.2 model of the arrival of particle radiation and a travelling shock at Venus on 6 December 2006 were verified by in-situ measurements made aboard Venus Express (VEX) by the ASPERA 4 instrument. Interplanetary scintillation observations, as well as the ENLIL 3-D MHD model when employed separately or in combination, enable the making of predictions of the solar wind density and speed at various locations in the inner heliosphere. Both methods, which outdate HAFv.2, are utilized in the present paper to predict (retrospectively) the arrival of the flare related, interplanetary propagating shock recorded at Venus on 6 December 2006 aboard VEX with a view to putting in place the facility to make very reliable space weather predictions for BC during both its Cruise Phase and when in the Hermean environment itself. The successful matching of the December 2006 predictions with in-situ signatures recorded aboard Venus Express provide confidence that the predictive methodology to be adopted will be appropriate to provide space weather predictions for BepiColombo during its Venus flybys and throughout the mission.

1. Introduction

The European Space Agency/ESA and the Japanese Space Agency/JAXA have collaborated since the year 2000 to send a space mission to Mercury, named in honour of the Italian space scientist Giuseppe (Bepi) Colombo. This mission, which is presently scheduled to be launched in 2018, features three elements namely: a carrier spacecraft (contributed by ESA) known as the ***Mercury Transfer Module*/MTM**; the ***Mercury Planetary Orbiter*/MPO** which is also contributed by ESA and the ***Mercury Magnetospheric Orbiter*/MMO**, which is provided by JAXA. The MTM will supply chemical power to the two hibernating orbiters as well as power the, on-board, solar electric propulsion system during the Cruise Phase of the mission.

1.1. The cruise phase

It is planned that the BepiColombo (BC) spacecraft will leave the Earth at a hyperbolic excess velocity of 3475 km/s, driven by a, low thrust, solar electric propulsion/ion system that will steadily propel the spacecraft along a series of arcs around the Sun. After two years BC will return to Earth to perform a gravity assist manoeuvre and be deflected towards planet Venus. The trajectory of the spacecraft will, thereafter, be modified through performing two Venus flybys (in 2019 and 2020 respectively) which will result in reducing, with almost no need for thrust, the pertaining perihelion distance to Mercury. Thereafter, a series of 5 Mercury flybys will result in lowering the relative velocity between Mercury and BepiColombo to 1.76 km/s. Finally, four thrust arcs will further reduce the relative velocity attained to a point where, on 18 December 2024 (following the jettisoning of the MTM from the spacecraft stack), BepiColombo will be captured by Mercury's gravity and perform a polar orbit around the planet.

MPO will next fire chemical propulsion thrusters to lower this orbit. Finally, MPO and MMO will be deployed into separate orbits (see

* Corresponding author.
E-mail address: stil@nuim.ie (S. McKenna-Lawlor).

https://doi.org/10.1016/j.pss.2017.10.001
Received 29 December 2016; Received in revised form 20 June 2017; Accepted 9 October 2017
Available online 13 October 2017

representative Fig. 1), in which they will carry out, at a range of separations, a program of closely co-ordinated observations of Mercury and its environment under the aegis of a collaborative agreement between the European and Japanese scientific teams.

The autonomous and co-ordinated observations carried out thereafter at Mercury over 1 Earth year (4 Mercury years), with the option of a one Earth year extension, will result in the most comprehensive investigation of Mercury and its environment hitherto undertaken (previous missions to Mercury were Mariner 10, launched in 1973 and Mercury Messenger, launched in 2004). Among the scientific objectives of the spacecraft of the BepiColombo mission are: an in-depth investigation of Mercury's exosphere - its composition and dynamics; a study of Mercury's magnetosphere - its structure and dynamics; an inspection of Mercury's magnetic field and observations designed to reveal Mercury's surface composition, made, in particular, at times when energetic solar particles impact the planet.

1.2. The solar cycle

Samuel Schwabe discovered in 1843 the (approximately) 11-year cycle of the growth and decay of sunspot numbers, which is generally recognized to be linked with the level of ongoing solar activity. Attempts to predict when the next sunspot cycle might occur and how strong it would be have, over the years, been made by many. It is currently recognized that 11-years is an average (some cycles are as short as 9 years while others are as long as 14 years). Further, the number of sunspots during a peak year (called sunspot maximum), can vary from as few as 50 to as many as 260. Further, the speed with which sunspot numbers rise to a maximum can be as long as 80 months for weaker sunspot cycles, but as short as 40 months for those that are the strongest ones. These observed variations, combined with statistical considerations, have resulted in the construction of several predictive schemes but all of them fail to produce accurate and detailed forecasts of the 'next' sunspot cycle.

In the case of the current cycle (Number 24), which spans the years 2008–2019, a study by Pesnell (2016) showed, on the basis of 105 individual forecasts of how many sunspots would be present during the peak year, that the predictions varied from as few as 40 to as many as 175, with an average of 106 ± 31. The number actually observed to be present at the 2014 peak was 116. Most of the predictions utilized in the investigation were based on simple statistical considerations and, what is rather required although as yet unavailable, are forecasts based on the physics of sunspot formation (see for instance a review of available dynamo models by Charbonneau (2010)).

Through combining helioseismological observations made aboard the SOHO spacecraft (see an account of the Michelson Doppler Imager utilized in Scherrer et al., 1995) with ground-based observations made by the Global Oscillations Network Group (GONG), two principal components of temporal magnetic field variation that occurred during solar cycles 21–24 were identified in full disk magnetograms that covered about 39% of data variance with $\sigma = 0.67$, (Zharkova et al., 2015). These components were attributed to two main magnetic waves travelling from opposite hemispheres with close frequencies and increasing phase shift. Mathematical analysis of the waves was demonstrated to yield predictions of solar activity on a millennium basis. These forecasts suggested that Cycle 25 might continue a trend of polar field decline observed to already be in progress during the last three sunspot cycles (see Fig. 2) and thus develop overall to be yet weaker than Cycle 24, with fewer than 100 spots.

Statistically speaking, if the number of spot-free days continues to increase over the period 2017–2018, it can be expected that the new sunspots of Cycle 25 will appear sometime in late 2019 when BepiColombo is scheduled to perform its first Venus flyby. Sunspot maximum is likely to occur in 2024 when the spacecraft is already at Mercury.

Further, sunspot magnetic field strengths have been in decline since 2000 and are already close to the threshold required to sustain sunspots on the solar surface. Some of the current forecasts suggest that solar cycle 25 will be completely absent while others suggest that a sunspot maximum equal to or greater than that of cycle 24 is still possible. Thus, the means to provide accurate predictions of future cycles and the creation of a reliable theory as to why the Sun exhibits cycles at all are unavailable.

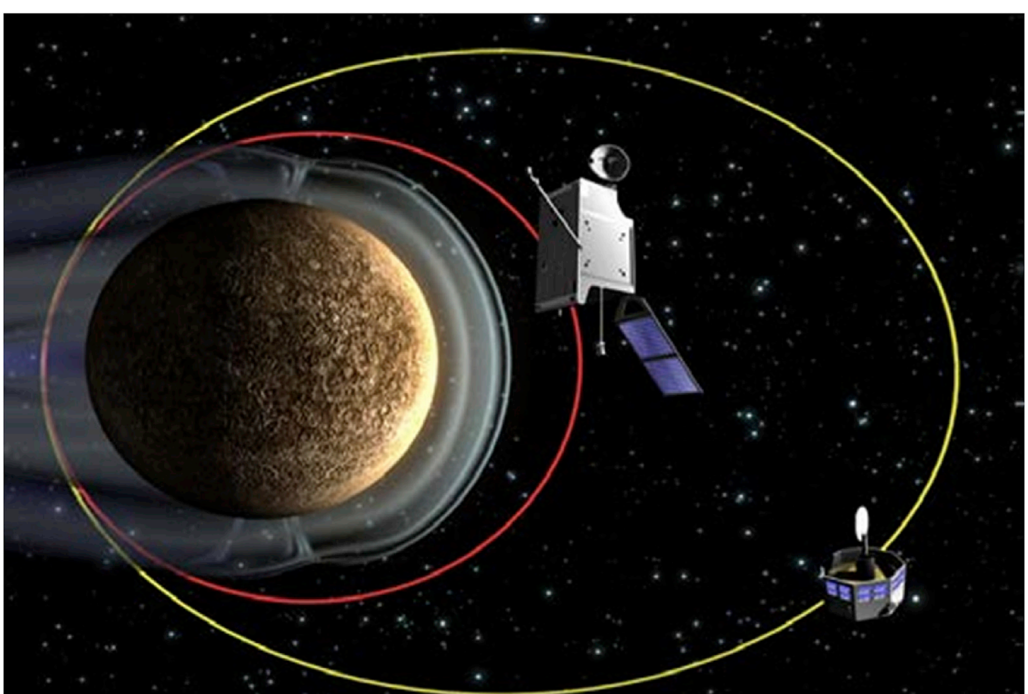

Fig. 1. Representative Orbits of MPO (red) and MMO (green, lower right) at Mercury.

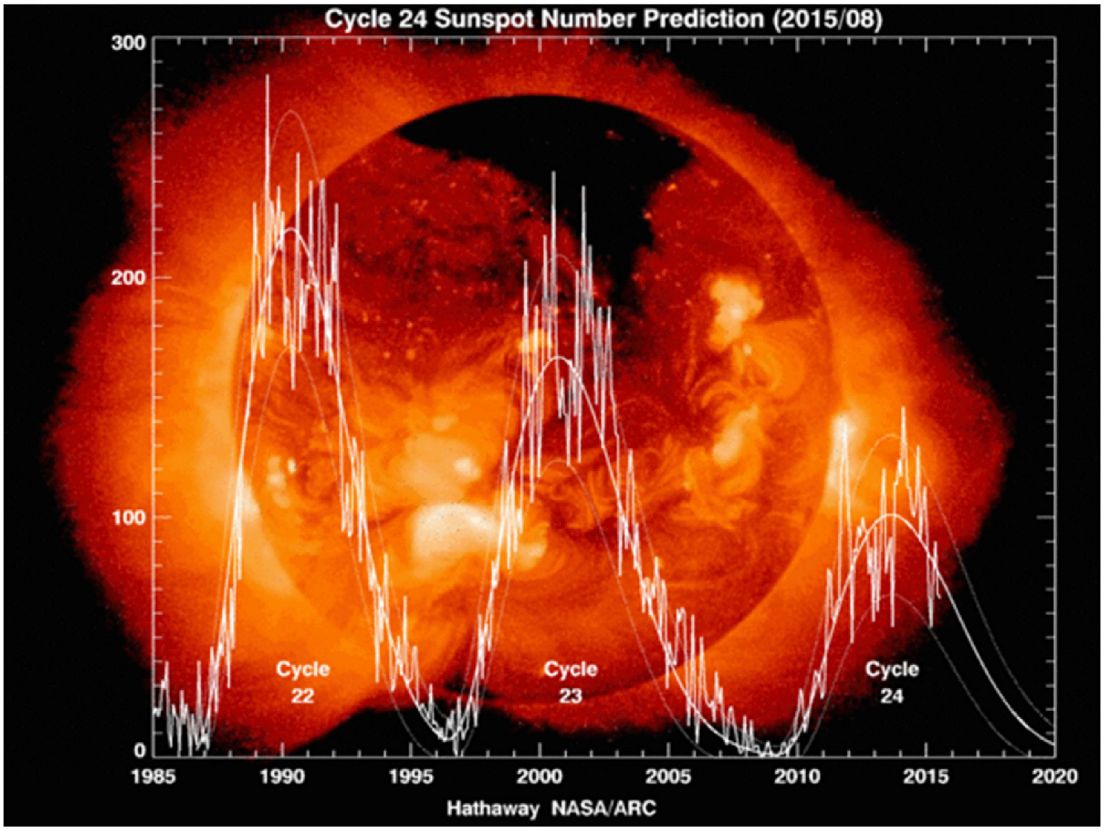

Fig. 2. Counts of sunspots recorded over the past few solar cycles. (Credit, NASA/ARC).

2. Space weather at Venus under conditions of solar cycle minimum

The arrival at Venus of significant solar disturbances while Bepi-Colombo is executing flybys of the planet would be expected to profoundly affect certain of the onboard measurements. Given that the flybys are scheduled to occur at around the time of the minimum of solar cycle 24 one might intuitively expect that the probability of the occurrence at this time of a large solar event would be very low. It should, however, be pointed out that, at the start of the minimum of previous solar cycle 23, major activity occurred in NOAA Active Region 0930.

On 5 December 2006 this region transited the solar east limb at 6° south latitude (S06). Thereafter, over the course of some nine days, it produced: four X-class flares. These peaked to X9.0 at Earth on 5 December at 10:35UT from S06E59; to X6.5 on 6 December at 18:47UT from S05E57; to X3.4 on 13 December at 02:40UT from S07W22, and to X1.5 on 14 December at 22:15UT from S06W46. Each of these events was accompanied by a metric Type II burst, thereby indicating the propagation through the solar corona on each occasion of a large shock. Fig. 3 shows the positions of the Earth, Venus and Mars http://cdaw.gsfc.nasa.gov/CME_list/daily_plots/sephtx/2006_05/sephtx_20060501.png relative to the Sun on 6 December 2006 when Earth was ~80° to the west and Mars ~125° to the east of the Sun. Venus and Mars were located at that time in the same general region of the Parker Spiral.

2.1. Numerical modelling of the arrival at Earth, of disturbances associated with the December 2006 events

Several numerical models which use solar observations as inputs to forecast the arrival at Earth of flare-related-shocks were available for use at the time of the December activity, among them the ***Hakamada-Akasofu-Fry version 2***/modified HAFv.2 model [Dryer et al., (2001, 2004); Fry et al., (2001, 2007); Smith et al., (2003, 2009)].

Application of the HAFv.2 model to the data showed, not illustrated here but available in McKenna-Lawlor et al. (2008), that during the very early part of the activity, a shock (designated S2), which was associated with the event of 6 December, was refracted and expanded to westward

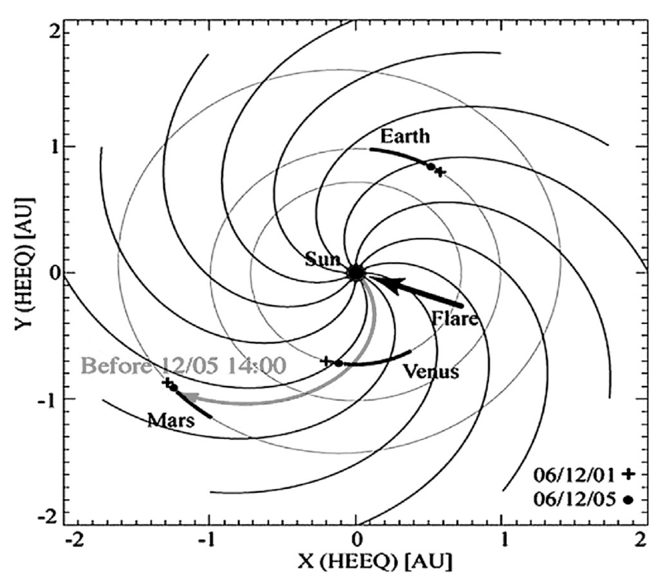

Fig. 3. Locations of the Earth, Venus and Mars relative to the Sun on 6 December 2006. The location of the flare on 6 December is indicated by an arrow. Venus was ~80° to the west and Mars ~125° to the east of the Sun and both of these planets were located on the same magnetic field line of an ideal Parker Spiral (following Futaana et al., 2008).

close to the Sun, after which it overtook and merged with a further shock (designated S1), which had been generated earlier in association with the flare of 5 December. The HAFv.2 model predicted the arrival at Earth of the western flank of the merged shock at ~07:00 UT on 8 December. Both the ACE/MAG (Magnetometer) and SOHO/MTOF (Mass Time Of Flight) instrument aboard SOHO recorded the arrival at L1 of this composite shock some 3 h earlier, after a 33 h transit time. HAFv.2 simulations were also made of the propagation of Shocks 3 and 4 from the site of their associated flares on December 13 and 14. The arrival of Shock 3 was recorded at L1 at 13:52 UT on 14 December while Shock 4 arrived at 17:21 UT on 16 December. The corresponding HAFv.2 model predictions were respectively within 8 min (0 h) and ~5 h of these measured shock arrivals after their (35 and 43 h) respective transit times from the Sun, [McKenna-Lawlor et al., (2008)]. In the parlance of HAFv.2 modelling all of these correspondences were HITS.

2.2. *Numerical modelling of the arrival at Venus and Mars of disturbances associated with the December 2006 event*

Shock/SEP signatures could be recorded at Venus and Mars in the background counts of the *Electron Spectrometer* (ELS) and of the *Ion Mass Analyzer* (IMA) experiments which form part of the *Analyzer of Space Plasma and Energetic Atoms*/ASPERA instrument suites installed aboard *Mars Express* (MEX/ASPERA-3/launch 2003) and *Venus Express* (VEX/ASPERA-4/launch 2005). Details concerning the MEX and VEX instruments are contained in [Barabash et al., (2006, 2007)].

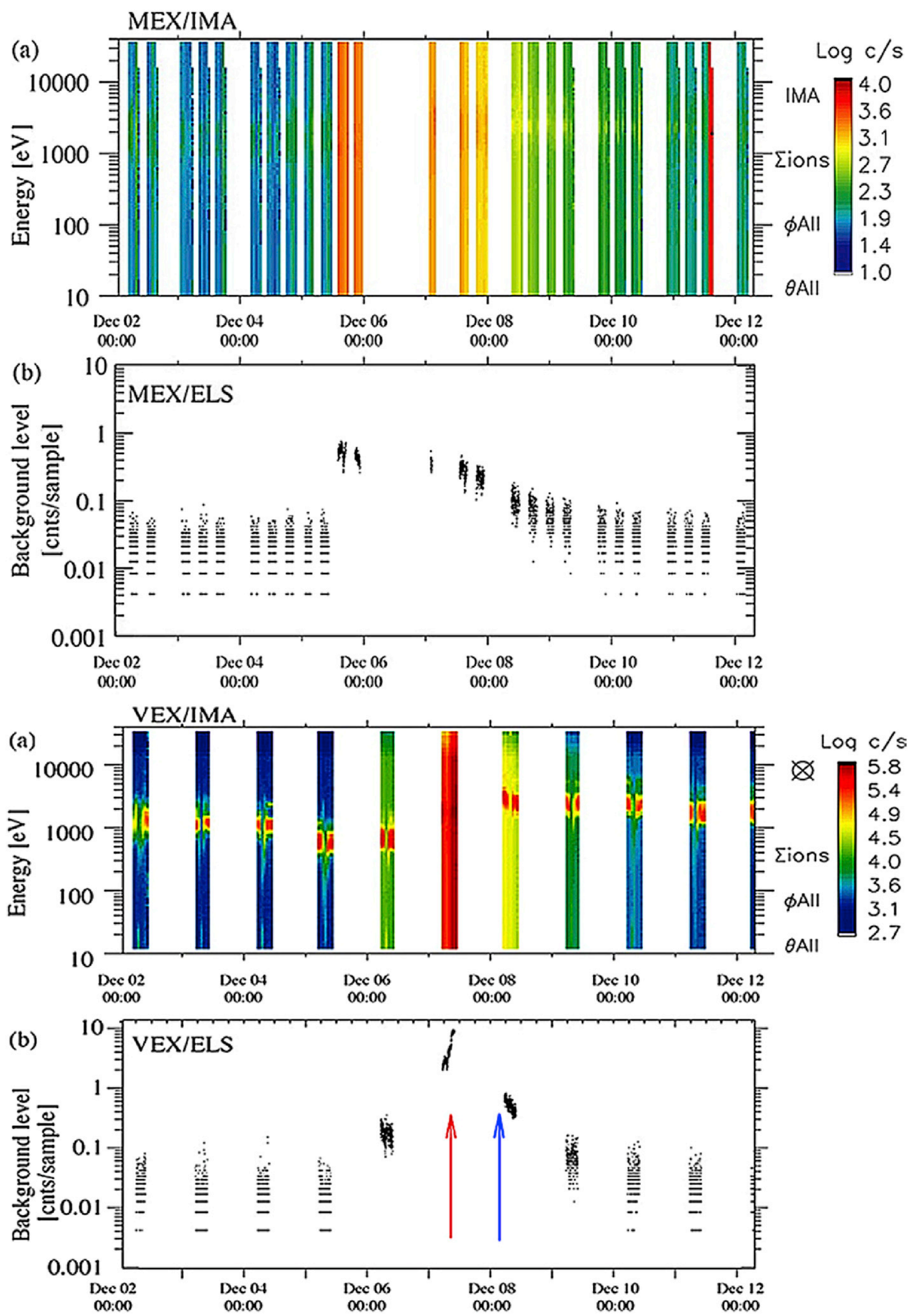

Fig. 4. (Panel 1, top) An energy–time spectrogram recorded at Mars by ASPERA-3/IMA in the interval 2-12 December 2006; (panel 2) corresponding total count rates in the highest 15 energy steps of ASPERA-3/ELS. (Panels 3-4) Complementary data recorded at Venus by ASPERA-4 IMA and ASPERA-4/ELS. For details see the text. In the bottom panel arrows indicate the location of a shock signature, McKenna-Lawlor et al. (2008).

Although neither the ELS nor IMA is designed to detect energetic protons, both can detect ambient, high-dose radiation (X-rays, γ-rays, MeV ions) through their capability in each case to register a high incidence of uniform background counts. These counts are produced due to the penetration of energetic particle radiation through the walls of both instruments where they impact on the micro-channel plates mounted within. The enhancement of background count levels thus recorded is independent of the energy steps of both ASPERA-3 and ASPERA-4 [Futaana et al. (2008); McKenna-Lawlor et al., (2008)].

Fig. 4 shows (second panel from the bottom) the energy-time spectrogram recorded by ASPERA-4/IMA at Venus from 2–12 December, 2006. In the bottom panel appears the corresponding total count rate measured in the highest 15 energy steps of ASPERA-3/ELS. Because the latter energy range is normally free from counts, the data recorded in this channel can be considered to constitute a proxy for the ambient particle background. This count rate was uniform in all $\pi \times 2\pi$ directions and its uniformity and long duration (3 days) all indicate that the background enhancement was caused by an SEP event (a solar X-ray or gamma-ray burst signature would not typically last for 3 days).

Although the exact starting time of the background level increase cannot be determined due to a data gap, its most likely source was the X9.0 flare on December 5, 2006, probably supplemented by the X6.5 flare in the same region on December 6, 2006. There was no other candidate source on the Sun due to the pertaining solar minimum conditions [Futaana et al. (2008); McKenna-Lawlor et al., (2008)]. It was predicted by HAFv.2 that a composite shock, formed through the superposition of S2 and S1, would arrive at Venus at ~04:00 UT on 8 December 2006 and the data recorded by ASPERA-4 shows (Fig. 4 bottom panel) the presence of a shock (signature emphasized by arrows) on 7 December at 09:00 UT i.e. approximately 19 h 'early' (again a HIT).

HAFv.2 further predicted that, beyond Venus, the eastern flank of composite Shock S1—S2 would decay to an MHD wave. No shock signature was thus expected to arrive at Mars and, in accord with this prediction, no shock signature was recorded there (see Fig. 4, panel 2) although an enhanced particle background was present. (It is noted that it cannot be excluded, due to gaps in the record, that a shock might have arrived at Mars that was missed). For S1—S2, utilization of HAFv.2 modelling was one of the best techniques available to provide predictions at that time (see Section 4).

In the case of the flares of 13–14 December, each of which was associated with a travelling shock (S3 and S4), HAFv.2 simulations clearly showed that these events were very weak and had decayed to MHD waves before they could arrive at Venus. It is thus explicable that, on this occasion no shock signature was recorded at that planet. The interaction and superposition of S3 and S4 thereafter was predicted to build a composite shock that would arrive at Mars at ~00:00 UT on 20 December 2006. McKenna-Lawlor et al. (2008) provided indirect evidence of the arrival of this event at Mars close to the predicted time.

3. Two state-of-the-art solar wind modelling prediction techniques

At the time of writing the HAFv.2 modelling technique had undergone some criticism (McKenna-Lawlor et al., 2012 inter alia) but has been outdated by the development of a plethora of more sophisticated models. These different modelling efforts include, in the United States, three-dimensional magnetohydrodynamic (3-D MHD) modelling such as 1) those from the University of Alabama, Huntsville (UAH) (Kim et al., 2012, 2014; and Pogorelov et al., 2012) who devised the (MS-FLUKSS) 3-D MHD model; 2) the Naval Research Laboratory group using a model now termed H3DMHD (Wu et al., 2007); 3) the University of Michigan group who have developed the BATS-R-US MHD model using the Solar Corona (SC) and Inner Heliosphere (IH) components of the Space Weather Modelling Framework (SWMF) (Toth et al., 2012); and 4) ENLIL (see Odstrcil and Pizzo, 1999a, 1999b). Several other groups around the world in Europe (EUHFORIA, Poedts, 2017), Japan (REPPU, Tanaka et al., 2015) and China (Feng et al., 2010) recently provide their own versions of 3-D MHD modelling analyses. Two near real time models currently operate to provide these analyses using IPS data. These models are from the Institute for Space Earth Environment (ISEE, formerly STELab) group (Hayashi et al., 2016), and UCSD IPS time-dependent modelling using the ISEE IPS data (Section 3.1 below).

For the BepiColombo mission it is intended that we will utilize two state-of-the-art models to predict the arrival of space weather at the spacecraft during its Cruise Phase and while orbiting Mercury. These two models, which are used at the NASA Community Coordinated Modelling Center (CCMC) and world-wide and have the longest heritage of use, are ENLIL and the UCSD modelling. Both have been developed to operate efficiently in near real time on relatively small computer systems, to provide CME predictions that compare successfully with in-situ measurements, and are continually updated as new data-handling, techniques and modelling innovations become available. The two chosen models are described below and their fitness tested against the in-situ measurements recorded at Venus aboard Venus Express (see above) in early December 2006.

3.1. The Interplanetary Scintillation 3-D reconstruction technique

The ***Interplanetary Scintillation 3-D reconstruction Technique*** (IPS analyses) which was developed in time-dependent form at the University of California, San Diego, provides precise tomographic 3-D reconstructions of the, time-varying, global heliosphere. The technique operates by iteratively fitting IPS observations to a kinematic solar wind model that conserves mass and mass flux. These analyses of transient solar wind features can match, as well as provide an extended low-resolution global view of, the solar wind parameters speed, density and vector magnetic fields extrapolated from the solar surface which are usually only measured by in-situ sensors (e.g., Jackson, 2011).

Used with, ISEE, Japan IPS observations (http://stesun5.stelab.nagoya-u.ac.jp/index-e.html), this technique has already been in operation since the year 2000 to predict conditions in real time in the inner heliosphere (see: http://ips.ucsd.edu). Solar data recorded during recent missions, (e.g., STEREO, SMEI), have significantly improved the possibility to remotely measure detailed aspects of specific solar transient events near the Sun, including their outflow, and 3-D structure. Such observations show increased solar wind detail that certifies, and can be compared with, the results of IPS analyses. Also, a real-time prediction of conditions at comet 67P/Churyumov-Gerasimenko, updated every 6 h, was produced and the resulting final predictions of the arrival at the comet of major solar related disturbances successfully compared with the corresponding onsets of disturbed magnetic and plasma signatures recorded in situ aboard the Rosetta spacecraft (McKenna-Lawlor et al., 2016).

3.2. The ENLIL (mesopotamian god of the wind) modelling tool

ENLIL is a time-dependent 3-D MHD model of the heliosphere which solves equations for: plasma mass; momentum and energy density; and magnetic field; using a Flux-Corrected-Transport (FCT) algorithm. Its inner radial boundary is typically located at 21.5 solar radii and it can accept boundary condition information from the Wang-Sheely-Arge/WSA model (Arge and Pizzo, 2000). Its outer radial boundary can be adjusted to include planets or spacecraft of interest (in the present case BepiColombo). It covers 60° north to 60° south in latitude and 360° in azimuth (Odstrcil et al., 1999a, 1999b). Both ENLIL and the kinematic 3-D reconstruction analysis can provide extractions at a point location over time from the volumetric data set anywhere within the volume. Under these circumstances it is anticipated that, at particular separations, it may be possible to differentiate between solar conditions recorded at MPO and MMO.

The IPS 3-D reconstruction results can also be extracted at any solar distance as two-dimensional maps over time within the reconstructed volume and may thus be exploited to provide inner boundary values to drive the ENLIL model either from archival data (Yu et al., 2015) or in near real time (Jackson et al., 2015).

4. Predictions using the IPS and ENLIL tools to determine the arrival of solar related disturbances at Venus in December 2006

For scientific studies after the fact, both the ENLIL and the IPS modelling analyses provide data from an inner boundary that is located at 0.1 AU and 15 solar radii (0.067 AU) respectively. Lower-resolution program versions of both the ENLIL and IPS models complete in about 20 min on modest multiple-node processors, and thus both provide adequate volumes for study within an hour of initiation from well-within the Mercury orbit. The normal cadence for near real time operation depends on several different factors. ENLIL can be initiated at any time following an alert of a significant solar event, and application of the modelling inputs. The IPS analysis depends both on IPS data being available and analysed at the data-taking site and, for slow CMEs, the ISEE data latency is only marginally adequate for Mercury near real time predictions, especially those using the IPS-driven ENLIL modelling. However, both modelling efforts continue to be updated for use in near-real-time. ENLIL used with cone model initiation techniques can be triggered to run automatically with data analysed using coronagraph observations. A large effort is underway from world IPS groups, a World Interplanetary Scintillation Stations network (WIPSS, Bisi et al., 2017), to combine IPS observations from around the world to help remove the long latency and low temporal coverage from daily-observed IPS data available from single IPS radio observatories. The current near-real-time IPS modelling is able to include these data whenever they become available in a standard format (Jackson et al., 2016).

Figs. 5–7 show the solar disturbances of 5 and 6 December 2006 modelled using the IPS technique. The analyses from 2006 are low resolution and do not show shock extents except by either an abrupt change in heliospheric density or velocity. Although many different data products are possible (see Jackson et al., 2010a, 2013, 2015) the volumetric cuts and time series are most often used to show results of these analyses.

In the case of 5 and 6 December 2006 X9.0 and X6.5 flares, there was preexisting heliospheric dense structure that bounded both the eastern and western flanks of the flaring region which was seen in particular near Venus, as shown in Fig. 5.

The large amount of dense material and very fast structure depicted to the east of the Sun at Earth's orbit is undoubtedly the enhanced plasma aftermath of these two events that was directed between Earth and Venus. As explained previously, this event was well-connected by pre-existing Parker spiral fields depicted in Fig. 3, and a conduit for the high energy particles of Fig. 4. Although this spiral field is shown by the tomography in Fig. 5, there is little evidence of a plasma density or velocity enhancement at Venus in the low-resolution time series tomographic

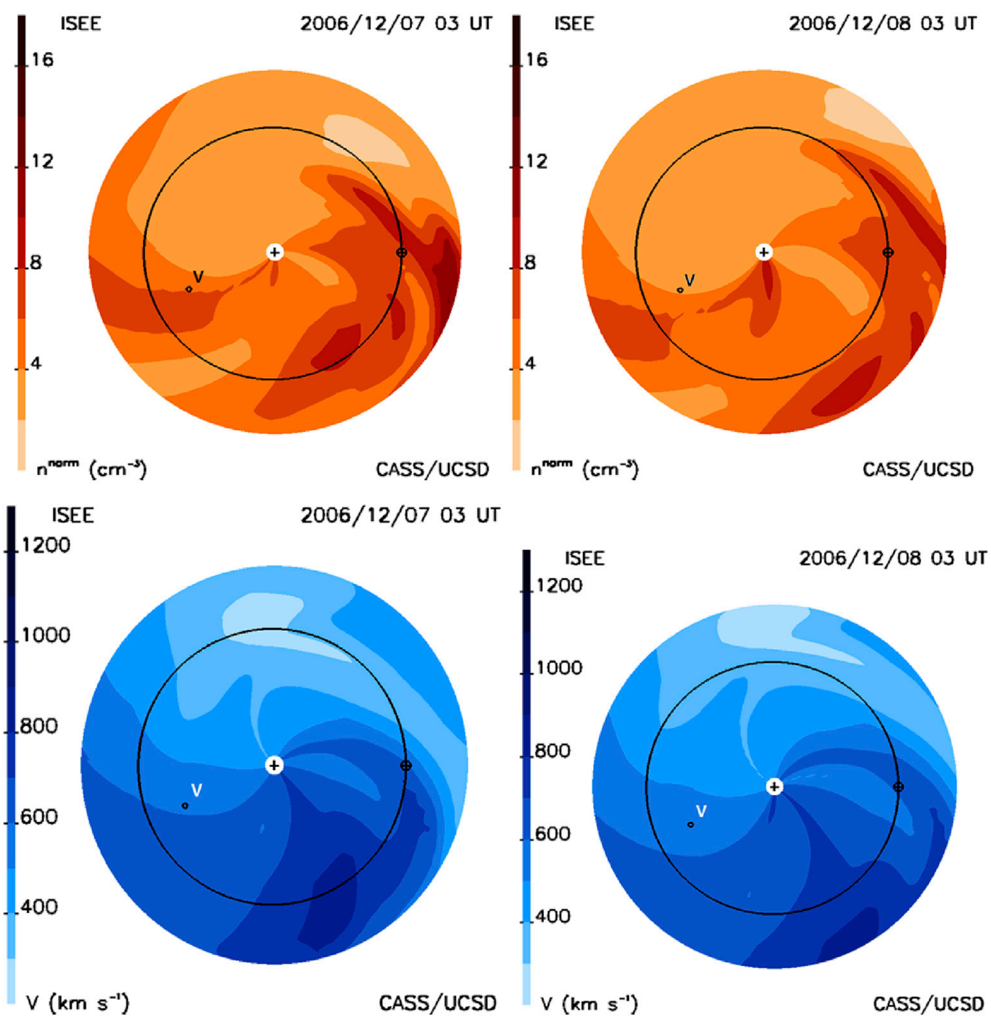

Fig. 5. An IPS-derived density ecliptic cut showing a portion of the plasma enhancement that is present at Venus at 03:00 UT on 7 December 2006, and also a day later on 8 December. Top panels: Density normalized to values at 1 AU; bottom panels: Radial velocity. The Sun is centred in the image with Earth positioned to the right on its orbit. The location of Venus is designated by a V.

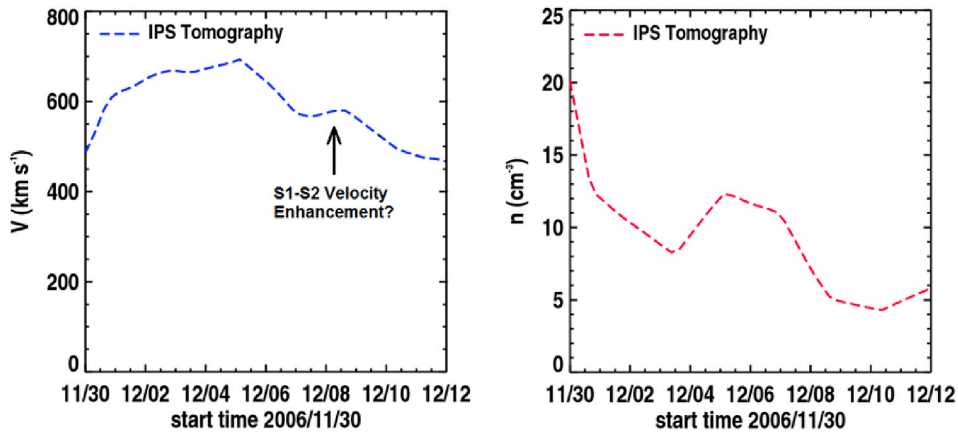

Fig. 6. Velocity and Density time series at Venus from 30 November to 12 December.

analysis at Venus, and there is little evidence of the shock that may have arrived at Venus from the eastern edge of the event as shown in Fig. 6. At Earth there is a different story. A pre-existing slow CME event has just passed Earth at 03 UT on 7 December as shown in Fig. 5, and depicted in the time series shown in Fig. 7. This feature commences at 1 AU prior to the X9.0 flare present at the solar west limb of the Sun observed from Earth. It is only by mid-day 8 December that the western flank of the combined S1—S2 events reaches Earth where it produces a plasma density enhancement. In the analysis shown in Fig. 7 the comparison Wind time series has been smoothed by a one-day boxcar average to make it commensurate with the low-resolution tomography available during this time period. However, there is little evidence of the S1—S2 shock velocity increase present in the velocity time series from aboard Wind, or from any of the other Earth-based monitors that could see this feature (ACE or CELIAS), even at the highest time resolutions.

Unfortunately, because of an outage following 04:06 UT on 4 December, there is no direct corroborating evidence from the LASCO coronagraphs of this earlier set of S1—S2 events. The aftermath of a very large and fast CME to the east and southeast of the Sun observed from Earth on 6 December was present when images from the C2 coronagraph resumed at 20:24 UT on 6 December, and this was undoubtedly associated with the S2 event. These two events have not been well-studied by using the ENLIL 3-D MHD modelling, primarily because there is no LASCO data to provide initiation inputs for these two extreme events, and

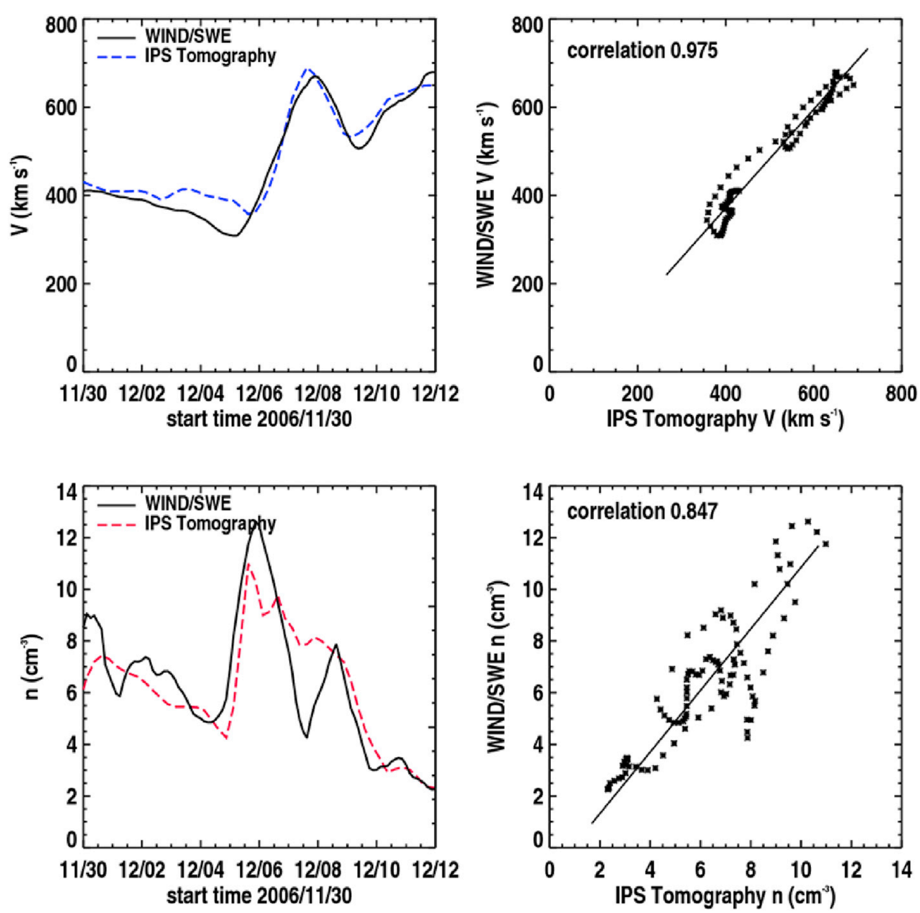

Fig. 7. Velocity and Density time series at Earth from 30 November to 12 December. Wind spacecraft in-situ measurements are compared.

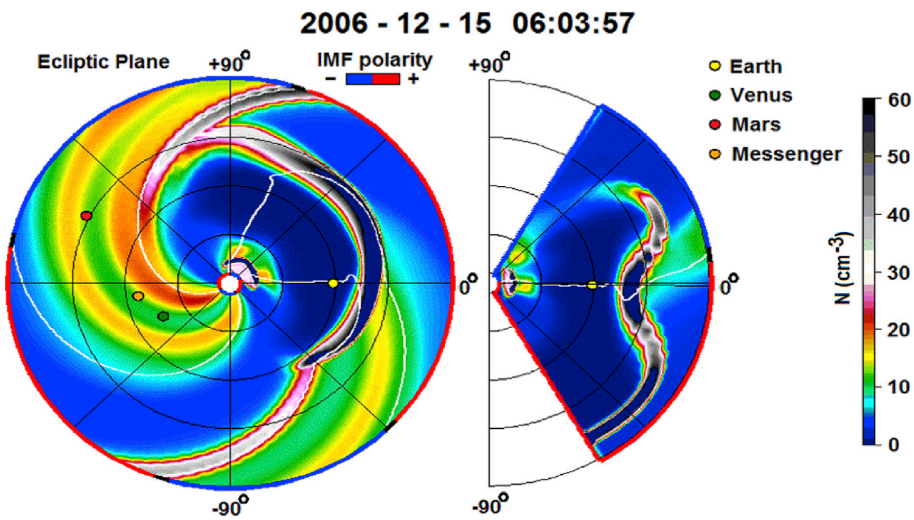

Fig. 8. WSA ENLIL analysis of the X3.4 flare and X1.5 flares and associated halo CMEs initiated on 13 and 14 December. An ecliptic cut of density normalized to values at 1 AU is on the left with a meridional cut of the same heliospheric structure is on the right. Positions of Earth, Venus, Mars and Messenger are indicated on the ecliptic plot.

thus only the IPS result shown here has been available to support an analysis.

However, the S3 and S4 events on 13 and 14 December have been well-studied by ENLIL 3-D MHD modelling. This is primarily because there have been LASCO data to provide "cone" inputs (e.g., Luhmann et al., 2010) to the ambient plasma parameters using WSA magnetic field analysis, and further because both events occurred near Sun center. Both X3.4 and X1.5 flares were associated with fast halo CMEs, the former listed with a speed of 1774 km/s and the latter with a speed of 1042 km/s in the SOHO/LASCO CME Catalog (Gopalswamy et al., 2009). Figs. 8 and 9 depict these two events in the ENLIL modelling. At the time indicated in Fig. 8, the CME associated with the X3.4 flare on 13 December at 02:40 UT from S07W22 has passed Earth, and the CME associated with the X1.5 flare on 14 December at 22:14 UT from S04W46 is just seen beginning its outward motion. In Fig. 9 the first event in the sequence has passed almost entirely beyond 2 AU, while the second event in the sequence has just reached Earth. There is no evidence in this modelling that either event has extended around to the location of Venus, which is situated nearly 180° from the location of both of the large flares in this sequence.

5. Modelled data availability

In 2006 [until the newer SWIFT radio array (Kojima et al., 2002; Tokumaru et al., 2011), a cylindrical parabola oriented north-south and steered electronically was commissioned in 2010], snow in Japan predicated closure of the large moveable radio arrays used to provide IPS data. Relative to the events described here, this closure occurred on 9 December 2006. Outward propagation of measurements obtained near the Sun allowed the analysis from this instrumentation to continue for a few days beyond that date, as shown in the time series of Figs. 6 and 7.

Since 2010, the UCSD time-dependent tomographic analysis has been operated year-round at UCSD in real time (see http://ips.ucsd.edu), at the NASA Goddard Community Coordinated Modelling Center (CCMC), and since 2014 at the Korean Space Weather Center (KSWC), Jeju, South Korea. The IPS analyses from ISEE, Japan instruments are best when events propagate slowly outward, because this allows several days of observation of them as they cross the line of sight on the way outward to the inner planets. Current efforts are now underway to incorporate other Worldwide IPS Stations (WIPSS) using the IPS tomography in a network to provide better coverage around the clock. In the near future this is

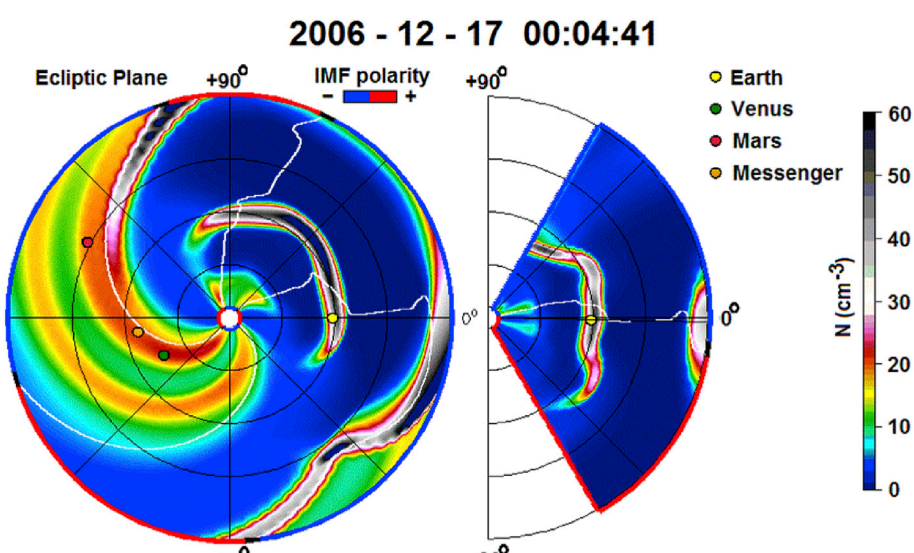

Fig. 9. WSA ENLIL analysis of the X1.5 flare and the associated halo CME initiated on 14 December. An ecliptic cut of density normalized to values at 1 AU is on the left with a meridional cut of the same heliospheric structure on the right. Positions of Earth, Venus, Mars and Messenger are indicated on the ecliptic plot.

expected to include IPS data from the Mexican Array Radio Telescope (MEXART), and the Pushchino, Russia, Big Scanning Array (BSA). When incorporated into the tomography, this will provide IPS coverage from different world longitudes as well as greater spatial and temporal volumetric resolutions.

Because the tomographic analysis is available at any height above the Sun, boundary conditions can be obtained for use to drive an ENLIL model using velocity, density and magnetic fields (Jackson et al., 2010b; Yu et al., 2015; Jackson et al., 2015; McKenna-Lawlor et al., 2016). This new technique has also been used to help predict CME outward propagation in real time at the KSWC, and at George Mason University, Virginia, USA since 2014, and provides some of the same benefits of both the iterative IPS analysis as well as the ENLIL modelling that can incorporate cone inputs.

6. Venus flyby measurements

On the Mercury Planetary Orbiter (MPO) only those instruments that are not obstructed by the Mercury Transfer Module (MTM), or not in need of pointing, can be operated during the Venus flybys. The experiments that will be active include: SERENA/MIPA - which will make measurements of: solar wind boundary crossings; pickup ions from the bow shock; ion escape flux and ionosphere composition and SERENA/PICAM – which will monitor: solar wind pickup ions; ion populations in the terminator/wake regions and in plasma boundaries (Milillo et al., 2010). Also, the SIXS spectrometer will be in operation which will monitor solar X-rays; energetic protons and electrons as well as detect SEP events (Khalid et al., 2009).

The Mercury Magnetosphere Orbiter (MMO) will be substantially shielded by a sunshade cone (MOSIF) during the cruise phase. Operational however will be the Mercury Plasma Particle Experiment MPPE/ENA instrument - which can detect energetic neutral atoms in the Venus environment and MPPE/HEP-ele., which can detect electron populations in selected keV ranges (Yoshiffumi et al., 2015).

During the flybys the above mentioned instrumentation will investigate, overall, details of the plasma structure and dynamic events in the Venus environment. The tools described in the present paper, with their capability to provide complementary background space weather information, will be essential in elucidating from the onboard measurements how the planet interacts with the solar wind.

It is noted that the tools described will be equally well suited to provide space weather observations yet further inside the heliosphere, in and around Mercury, which may provide an interesting supplement to comparable studies planned by a parallel ESA mission (Solar Orbiter) and by NASA's Solar Probe.

7. Discussion

The extrapolation of activities in 2006 to similar activities in 2019 is arguable since present indications suggest (Section 1.2) that this period will provide fewer opportunities to witness extreme events than was the case during solar cycle 23 (e.g., Zharkova et al., 2012, 2015; Shepherd et al., 2014). However, although various researchers are trying to push the limits of prediction ever further using statistical and dynamical models together with some data based intuition, knowledge of the next solar cycle is presently so limited that what will actually happen remains a matter for open speculation. In any case, effects of various events will be observed in the different planetary environments studied by the BepiColombo spacecraft, and this modelling effort will address the solar wind in-situ manifestations of the smaller events as well as those that are more extreme.

8. Conclusions

The BepiColombo/BC spacecraft (to be launched in 2018) will perform two flybys of Venus during its Cruise Phase to Mercury. At Mercury BC will perform 5 flybys of the planet, following which its two on-board spacecraft MPO and MMO will execute separate trajectories so that they orbit Mercury at various separations from each other. The flybys of Venus and Mercury will be performed during the minimum of solar cycle 24 but it cannot be excluded, based on the occurrence of four major solar events at the minimum of solar cycle 23, that significant solar flares and CMEs will be generated at this time. Further, significant solar events may occur during the (1–2 year) planet-orbiting phase of BepiColombo.

IPS modelling can provide low-resolution velocity and density forecasts of the arrival at selected heliospheric locations of time-variable heliospheric structures, as depicted in the examples shown. When data from the WIPSS network are available in early 2018, they will support IPS analyses of the fastest CME events, at higher spatial and temporal resolution.

ENLIL using the cone model and WSA inputs can track travelling CME driven shocks for even the fastest events. With boundary conditions provided by the IPS, the advantage of being able to track the fastest CMEs combined with the iterative capability of the IPS, can be used to refine the outward motion of these events.

Predictions of the IPS model regarding the arrival at specific heliospheric locations of solar disturbances was herein tested by applying this tool to predict the arrival of the S1 and S2 events at Venus and at Earth recorded in situ at these locations in early December 2006. The ENLIL modelling shows in addition that the S3 and S4 events generated in mid-December which produced no recorded signatures at Venus, could not have been observed at this time through changing plasma velocity and density because the planet was too far around the Sun from the flare and CME location. These predictions are entirely consistent with the results of earlier HAFv.2 modelling performed by McKenna-Lawlor et al. (2008), but they lend far more credence to them.

Thus the use of available IPS and ENLIL modelling to predict the arrival of space weather at the BepiColombo spacecraft is appropriate. These analyses are expected to increase significantly in accuracy over the next year.

Acknowledgements

B. Jackson, has been partially funded by AFOSR contract FA9550-15-1-0477 and NSF contract AGS-1358399 to the University of California, San Diego. We thank M. Tokumaru of ISEE, Nagoya University, Japan for making available the ISEE IPS observations used in a portion of this analysis.

References

Arge, C.N., Pizzo, V.J., 2000. Improvement in the prediction of solar wind conditions using near real time solar magnetic field updates. J. Geophys. Res. 105, 10,465–10,480.

Barabash, S., Lundin, R., Andersson, H., Brinkfeldt, K., Grigoriev, A., Gunell, H., Holmström, M., Yamauchi, M., Asamura, K., Bochsler, P., Wurz, P., Cerulli-Ielli, R., Mura, A., Milillo, A., Maggi, M., Orsini, S., Coates, A.J., Linder, D.R., Kataria, D.O., Curtis, C.C., Hsieh, K.C., Sandel, B.R., Frahm, R.A., Sharber, J.R., Winningham, J.D., Grande, M., Kallio, E., Koskinen, H., Riihelä, P., Schmidt, W., Säles, T., Kozyra, J.U., Krupp, N., Woch, J., Livi, S., Luhmann, J.G., McKenna-Lawlor, S., Roelof, E.C., Williams, D.J., Sauvaud, J.-A., Fedorov, A., Thocaven, J.-J., 2006. The analyser of space plasmas and energetic atoms (ASPERA-3) for the Mars express mission. Space Sci. Rev. 126, 113–164.

Barabash, S., Sauvaud, J.-A., Gunell, H., Andersson, H., Grigoriev, A., Brinkfeldt, K., Holmström, M., Lundin, R., Yamauchi, M., Asamura, K., Baumjohann, W., Zhang, T.L., Coates, A.J., Linder, D.R., Kataria, D.O., Curtis, C.C., Hsieh, K.C., Sandel, B.R., Fedorov, A., Mazelle, C., Thocaven, J.-J., Grande, M., Koskinen, Hannu E.J., Kallio, E., Säles, T., Riihela, P., Kozyra, J., Krupp, N., Woch, J., Luhmann, J., McKenna-Lawlor, S., Orsini, S., Cerulli-Irelli, R., Mura, M., Milillo, A., Maggi, M., Roelof, E., Brandt, P., Russell, C.T., Szego, K., Winningham, J.D., Frahm, R.A., Scherrer, J., Sharber, J.R., Wurz, P., Bochsler, P., 2007. The analyser of space plasmas and energetic atoms (ASPERA-4) for the Venus express mission. Planet. Space Sci 55 (12), 1,772–1,792.

Bisi, M.M., Americo-Gonzalez-Esparza, J., Jackson, B., Aguiliar-Rodriguez, E., Tokumaru, M., Chashei, I., Tyul'bashev, S., Manoharan, P., Fallows, R., Chang, O., Yu, H.-S., Fujiki, K., Shishov, V., Bards, D., 2017. The Worldwide interplanetary scintillation (ips Stations (WIPSS)) network in support of space-weather science and forecasting. Geophys. Res. Abstr. 19, EGU2017–13454.

Charbonneau, P., 2010. Dynamo models of the solar cycle. In: Living Reviews in Sol. Phys, vol. 7. http://www.livingreviews.org/lrsp-2010-3.
Dryer, M., Fry, C.D., Sun, W., Deehr, C.S., Smith, Z., Akasofu, S.-I., Andrews, M.D., 2001. Prediction in real-time of the 2000 July 14 heliospheric shock wave and its companions during the 'Bastille epoch'. Sol. Phys. 204, 265–284. https://doi.org/10.1023/1014200719867.
Dryer, M., Smith, Z., Fry, C.D., Sun, W., Deehr, C.S., Akasofu, S.-I., 2004. Real-time shock arrival predictions during the "Halloween 2003" epoch. Space Weather, S09001. https://doi.org/10.1029/2004SW000087.
Feng, X., Yang, L., Xiang, C., Wu, S.T., Zhou, Y., Zhong, D., 2010. Three-Dimensional solar wind modeling from the Sun to Earth by a SIP-CESE MHD model with a six-component grid. Astrophys. J. 723, 300–319.
Fry, C.D., Sun, W., Deehr, C.S., Dryer, M., Smith, Z., Akasofu, S.-I., Tokumaru, M., Kojima, M., 2001. Improvements to the HAF solar wind model for space weather predictions. J. Geophys. Res. 106 (A10), 20,985–21,001.
Fry, C.D., Detman, T.R., Dryer, M., Smith, Z., Sun, W., Deehr, C.S., Akasofu, S.-I., Wu, C.C., McKenna-Lawlor, S., 2007. Real-time solar wind forecasting: capabilities and challenges. J. Atmosph. Solar-Terr. Phys. 69, 109–115.
Futaana, Y., Barabash, S., Yamauchi, M., McKenna-Lawlor, S., Lundin, R., Luhmann, J.G., Brain, D., Carlsson, E., Sauvaud, J.-A., Winningham, J.D., Feahm, R.A., Wurz, P., Holtström, M., Gunell, H., Kallio, V., Baumjohann, W., Lammer, H., Sharber, J.R., Hsieh, K.C., Andersson, H., Grigoriev, A., Brinkfeldt, K., Nilsson, H., Asamura, K., Zhang, T.L., Coates, A.J., Linder, D.R., Cataria, D.O., Curtis, C.C., Sandel, B.R., Fedorov, A., Mazelle, C., Thocaven, J.-J., Grande, M., Koskinen, Hannu E.J., Sales, T., Schmidt, W., Riihela, P., Kozyra, J., Krupp, N., Woch, J., Franz, M., Dubinin, E., Orsini, S., Cerulli-Irellis, R., Mura, A., Milillo, A., Maggi, M., Roelof, E., Brandt, P., Szego, K., Scherrer, J., Bochsler, P., 2008. Mars Express and Venus express multi-point observations of geoeffective solar flare events in December 2006. Planet. Space Sci. 56 (issue 6), 873–880.
Gopalswamy, N., Yashiro, S., Michaleck, G., Stenborg, G., Vourlidas, A., Freeland, S., Howard, R., 2009. The SOHO/LASCO CME catalog. Earth Moon Planets 104, 295–313.
Hayashi, K., Tokumaru, M., Fujiki, K., 2016. MHD-IPS analysis of relationship among solar wind density, temperature, and flow speed. J. Geophys. Res. 121, 7367–7384.
Jackson, B.V., 2011. The 3D analysis of the heliosphere using interplanetary scintillation and Thomson-scattering observations. Adv. Geosciences 30, 69–91.
Jackson, B.V., Hick, P.P., Bisi, M.M., Clover, J.M., Buffington, A., 2010a. Inclusion of in-situ velocity measurements into the UCSD time-dependent tomography to constrain and better-forecast remote-sensing observations. Sol. Phys. 265, 245–256.
Jackson, B.V., Buffington, A., Hick, P.P., Clover, J.M., Bisi, M.M., Webb, D.F., 2010b. The 26 April 2008 CME: SMEI 3-D reconstruction of an ICME interacting with a co-rotating solar wind density enhancement. Astrophys. J. 724, 829–834.
Jackson, B.V., Clover, J.M., Hick, P.P., Buffington, A., Bisi, M.M., Tokumaru, M., 2013. Inclusion of real-time in-situ measurements into the UCSD time-dependent tomography and its use as a forecast algorithm. Sol. Phys. 285, 151–165.
Jackson, B.V., Odstrčil, D., Yu, H.-S., Hick, P.P., Buffington, A., Mejia-Ambriz, J.C., Kim, J., Hong, S., Kim, Y., Han, J., Tokumaru, M., 2015. The UCSD kinematic IPS solar wind boundary and its use in the ENLIL 3-D MHD prediction model. Space Weather 13, 104–115. https://doi.org/10.1002/2014SW001130 (2015).
Jackson, B.V., Yu, H.-S., Hick, P.P., Buffington, A., Tokumaru, M., Gonzalez-Esparza, A., Mejia-Ambriz, J., Chang, O., Odstrcil, D., Hong, S., Kim, J., Lee, B., Yi, J., Yun, J., Bisi, M.M., 2016. UCSD ips time dependent tomography. In: Oral Presentation at the UCSD IPS Workshop Held 18–21 December at UCSD. La Jolla (online at). ftp://cass185.ucsd.edu/Presentations/2016_12_IPS_Workshop/Jackson/.
Khalid, F.F., Prydderch, M.L., Morrissey, Q., Seller, P., Valtonen, E., Peltonen, J., Syrjäsuo, M., Vainio, R., Huovelin, J., 2009. Solar Intensity X-ray Spectrometer (SIXS), ASIC for a large dynamic range onboard BepiColombo ESA mission to Mercury. In: IEEE Nuclear Science Symposium Conference Record N35-5.
Kim, T.K., Borovikov, S.N., Pogorelov, N.V., Yu, H.-S., Clover, J.M., Jackson, B.V., 2012. Time-dependent MHD simulations of the solar wind outflow using interplanetary scintillation observations. In: Hu, Q., Li, G., Zank, G.P., Ao, X., Verkhoglyadova, O., Adams, J.H. (Eds.), *AIP Conference Proceedings*, 1500, Space Weather: the Space Radiation Environment, 11th Annual International Astrophysics Conference (CSPAR) Palm Springs, pp. 140–146. CA 19-23 March.
Kim, T.K., Pogorelov, N.V., Borovikov, S.N., Jackson, B.V., Yu, H.-S., Tokumaru, M., 2014. MHD heliosphere with boundary conditions from a tomographic reconstruction using interplanetary scintillation data. J. Geophys. Res. 119, 7981. https://doi.org/10.1002/2013JA019755.
Kojima, M., Tokumaru, M., Fujiki, K., Ishida, Y., Ohmi, T., Hayashi, K., Yamashita, M., 2002. Solar wind imaging facility for space weather research. Proc. SPIE 2002 (4853), 121. Waikoloa, 22-28 August.
Luhmann, J.G., Ledvina, S.A., Odstrcil, D., Owens, M.J., Zhao, X.-P., Liu, Y., Riley, P., 2010. Cone model-based SEP event calculations for applications to multipoint observations. Adv. Space Res 46, 1–21.
McKenna-Lawlor, S.M.P., Dryer, M., Fry, C.D., Smith, Z.K., Intriligator, D.S., Courtney, W.R., Deehr, C.S., Sun, W., Kecskemety, K., Kudela, K., Balaz, J., Barabash, S., Futaana, Y., Yamauchi, M., Lundin, R., 2008. Predicting interplanetary shock arrivals at Earth, Mars and Venus: a Real-time modelling experiment following the flares of 5–14 December, 2008. J. Geophys. Res. vol. 113, A06101 https://doi.org/10.1029/2007 JA012577.
McKenna-Lawlor, S.M.P., Ip, W., Jackson, B., Odstrcil, D., Nieminen, P., Evans, H., Burch, J., Mandt, K., Goldstein, R., Richter, I., Dryer, M., 2016. Space weather at comet 67P/churyumov-gerasimenko before its perihelion. Earth Moon Planets 117 (issue 1), 1–22.
McKenna-Lawlor, S.M.P., Fry, C.D., Dryer, M., Heyndericks, D., Kecskemety, K., Kudela, K., Balaz, J., 2012. A statistical study of the performance of the Hakamada-Akasofu-Fry version 2 numerical model in predicting solar shock arrival times at Earth during different phases of solar cycle 23. Ann. Geophys. 30, 404–419.
Milillo, A., Fujimoto, M., Kallio, E., Kameda, S., Leblanc, F., Narita, Y., Cremonese, G., Laakso, H., Laurenza, M., Massetti, S., McKennaLawlor, S., Mura, A., Nakamura, R., Omura, Y., Rothery, D.A., Seki, K., Storini, M., Wurz, P., Baumjohann, W., Bunce, E., Kasaba, Y., Helbert, J., Sprague, A., 2010. The BepiColombo mission: an outstanding tool for investigating the Hermean environment Planet. Space Sci. 56, 40–60.
Odstrcil, D., Pizzo, V.J., 1999a. Three dimensional propagation of CMEs in a structured solar wind flow,CME launched 1. CME launched within the streamer belt. J. Geophys. Res. 104, 483–492.
Odstrcil, D., Pizzo, V.J., 1999b. Three dimensional propagation of coronal mass ejections on a structured solar wind flow, 2. CME launched adjacent to the streamer belt. J. Geophys. Res. 104, 493–504.
Pesnell, W.D., 2016. Predictions of solar cycle 24: how are we doing? Space Weather 14 (1), 10–21. https://doi.org/10.1002/2015sw001304.
Poedts, S., 2017. EUHFORIA, State-of-the-art, Oral Contribution at EGU, vol. 2017, pp. 23–28. April, Vienna, Austria.
Pogorelov, N., Borovikov, S., Ebert, R., Jackson, B., Kim, T., Linker, J., Wu, S.-T., Zank, G., 2012. Modeling Heliosheath Flow with Observational Boundary Conditions, Paper Presented at the 39th COSPAR Scientific Assembly. Mysore, India, 14–22 July, (2010).
Scherrer, P.H., Bogart, R.S., Bush, R.I., Hoeksema, J.T., Kosovichev, A.G., Schou, J., Rosenberg, W., Springer, L., Tarbell, T.D., Title, A., Wolfson, C.J., Zayer, I., MDI Engineering Team, 1995. The solar Oscillations investigation- Michelson doppler imager. Sol. Phys. 162 (1–2), 129–188.
Shepherd, S.J., Zharkov, S.I., Zharkova, V.V., 2014. Prediction of solar activity from solar background magnetic field variations in cycles 21-23. Astrophys. J. 795, 46. https://doi.org/10.1088/0004-637X/795/1/46.
Smith, Z., Murtagh, W., Detman, T.R., Dryer, M., Fry, C.D., Wu, C.-C., June 23-28, 2003. Study of solar-based inputs into space weather models that predict interplanetary shock arrivals at Earth. In: Proc. SCOSTEP Int. Sol. Cycle Stud. Symp. ESA SP-535 (Publ. Noordwijk, The Netherlands), Tatranska, Lomnica, Slovakia, pp. 547–552.
Smith, Z.K., Dryer, M., McKenna-Lawlor, S.M.P., Fry, C.D., Deehr, C.S., Sun, W., 2009. Operational validation of HAFv2's predictions of interplanetary shock arrivals at Earth: declining Phase of Solar Cycle 23. J. Geophys. Res. 114, A05106 https://doi.org/10.1029/2008 JA013836.
Tokumaru, M., Kojima, M., Fujiki, K., Maruyama, K., Maruyama, Y., Ito, H., Iju, T., 2011. A newly developed UHF radiotelescope for interplanetary scintillation observations: solar Wind Imaging Facility. Radio Sci. 46, RS0F02.
Tanaka, T., Kubo, Y., Watari, S., 2015. REPPU (REProduce Plasma Universe) code for space weather simulators developed at NICT: 3-dimensional MHD simulation codes for the solar surface and global solar wind structure. In: Presentation at the 13–17 April NOAA Space Weather Workshop.
Toth, G., van der Holst, B., Sokolov, I.V., de Zeeuw, D.L., Gombosi, T.I., Fang, F., Manchester, W.B., Meng, X., Najib, D., Powell, K.G., Stout, Q.F., Glocer, A., Ma, A.Y.-J., Opher, M., 2012. Adaptive numerical algorithms in space weather modeling. J. Comput. Phys. 231 https://doi.org/10.1016/j.jcp.2011.02.006.
Wu, C.-C., Fry, C.D., Wu, S.T., Dryer, M., Liou, K., 2007. Three-dimensional global simulation of interplanetary coronal mass ejection propagation from the Sun to the heliosphere: solar event of 12 May 1997. J. Geophys. Res. 112 (A09104).
Yoshiffumi, S., Masafumi, H., Barabash, S., Dominique, D., Nicolas, A., Takeshi, T., Razushi, A., 2015. Current status of MPPE (Mercury plasma particle experiment on BepiColombo/MMO). In: Proc. EGU General Assembly 2015, Held 12-17 April 2015 in Vienna, Austria, 15573.
Yu, H.-S., Jackson, B.V., Hick, P.P., Buffington, A., Odstrčil, D., Wu, C.-C., Davies, J.A., Bisi, M.M., Tokumaru, M., 2015. 3D reconstruction of interplanetary scintillation (ips) remote-sensing data: global solar wind boundaries for driving 3d-MHD models. Sol. Phys. 290 (9), 2519–2538. https://doi.org/10.1007/s11207-015-0685-0.
Zharkova, V.V., Shepherd, S.J., Zharkov, S.I., 2012. Principal component analysis of background and solar magnetic field variations during solar cycles 21-23. Mon. Not. Roy. Astron. Soc. 424, 2943–2953.
Zharkova, V.V., Shepherd, S.J., Popova, E., Zharkov, S.I., 2015. Heartbeat of the Sun from principal component analysis and prediction of solar activity on a millennium timescale. Nature, 15689. Scientific Reports 5.